

Reaction of Nitrides of Molybdenum and Tungsten with Hydrogen Peroxide to Form Inorganic Proton Conductors

Hitoshi Nakajima, Hitoshi Tanaka, Mitsuhiro Hibino, Tetsuichi Kudo, and Noritaka Mizuno^{*,†}

Institute of Industrial Science, The University of Tokyo, Roppongi, Minato-ku, Tokyo 106

[†]Department of Applied Chemistry, Graduate School of Engineering, The University of Tokyo, Hongo, Bunkyo-ku, Tokyo 113

(Received October 22, 1997)

Reactions of nitrides of Mo, W, V, and Ti with hydrogen peroxide, especially Mo and W, were investigated. The reactions were characterized by elemental analysis, NMR, IR, Raman, XPS, TOF mass, and TG/DTA spectroscopy and titration of ammonia and peroxo group. The major oxometalate species in reaction solution for Mo and W were $[\text{MoO}(\text{O}_2)_2(\text{OOH})]_2^{2-}$ and $[\text{W}_2\text{O}_3(\text{O}_2)_4(\text{H}_2\text{O})_2]^{2-}$, respectively. As for the nitrogen-containing species, ammonium ions were initially formed, followed by the nitrate ions. Protons formed by the reaction take part in the formation of ammonia. The removal of unreacted hydrogen peroxide and the evaporation to dryness resulted in the formation of isopolymetalates. The peroxooctamolybdate, peroxododecatungstate, and decavanadate were suggested to be formed. Among them, the peroxopolytungstate was the most thermally stable and provided homogeneous thin films. The films showed protonic conductivity and the logarithm of conductivity changed linearly with the relative humidity or the inverse of the temperature.

Solid inorganic metal nitrides have attracted attention in the field of inorganic chemistry because many nitrides have novel compositions and coordination environments.^{1–5)} Some of them showed high stability to thermal and mechanical treatments and specific surface reactivity.^{6–8)} Therefore, they have been applied to material science,^{6–12)} catalysis,^{13–19)} and so on. However, much less is known of the reactivity of solid inorganic metal nitrides having atomic nitrogen at an interstitial position, except that some nitrides are chemically quite inert or those do react tend to decompose and hydrolyze to give corresponding metal hydroxides and ammonia, respectively.^{1,6–8)} It is also shown that the surface reactivity of nitrides with hydrogen sulfide is important for the catalytic hydrodenitrogenation.¹³⁾

In addition, the reaction of molybdenum, tungsten, vanadium, and titanium metals, carbides, and nitrides with hydrogen peroxide formed unknown amorphous peroxo-metalates,^{20–25)} and the resulting solid peroxo compounds have attracted much attention because of their applicability to inorganic precursors to proton conductors,^{26,27)} photoresists,²⁸⁾ electrochromic devices,^{29–31)} and metal oxides of hexagonal tungsten trioxide,³²⁾ tungsten bronzes,^{33–36)} and vanadium dioxide.³⁷⁾ The investigation of the solution chemistry as well as the produced inorganic precursors themselves are important for the better understanding.³⁸⁾ On the other hand, to date the reactivity of organometallic compounds of Mo with dinitrogen ligands has extensively been studied and ammonia, hydrazine, and dinitrogen have been identified as products.^{39–42)} However, almost nothing is known about formation of nitrate ions even for the reactions of these organometallic compounds.

In this report, we investigated the reaction solution of inorganic nitrides of molybdenum, tungsten, vanadium, and titanium with hydrogen peroxide, and we characterized the solid inorganic precursors formed by the reactions. In addition, the protonic conductivity of the most stable peroxopolytungstates was studied.

Experimental

Reagents. Nitrides of metals of Mo, W, V, and Ti (High Purity Chemicals), 30% aqueous hydrogen peroxide (Junsei Chemical), 0.01 M aqueous NaOH (1 M = 1 mol dm⁻³), and 0.002 M aqueous KMnO₄ (Wako Pure Chemicals) were commercially obtained and used without further purification.

Reaction with Hydrogen Peroxide. The reaction of metal nitride with hydrogen peroxide was carried out as follows: (1) Finely powdered solid metal nitride (200 mesh; 2 g) was added to an aqueous solution (200 ml) of hydrogen peroxide (15%, 0.94 mol). The solution was kept at room temperature for 24 h (final pH = 2.0). The solution was filtered to remove unreacted metal nitride. (2) Then Pt net was put into the solution to decompose excess hydrogen peroxide. The resulting solution was evaporated to dryness at 33 ± 2 °C. Finally the powder was dried in vacuo at room temperature for 12 h. The powder samples were used for the characterization. These samples prepared from nitrides of molybdenum, tungsten, vanadium, and titanium were abbreviated by (I), (II), (III), and (IV), respectively. The yields of (I)–(IV) were 88, 85, 16, and 6%, respectively.

Characterization. Infrared spectra were measured as KCl pellets with a Perkin–Elmer Paragon 1000 PC spectrometer. The NMR spectra of samples (solvent, D₂O; 27 °C) were recorded on JEOL-GX 270 FT spectrometer using liquid ammonia as a reference. X-Ray photoelectron spectra were recorded for self-supporting discs with a JEOL JPS-90SX spectrometer using a Mg Kα

source (1253.6 eV). The binding energies were corrected by using the value of 285.0 eV for the C 1s peak resulting from carbon contamination. Raman and TOF-MASS spectra were measured with T-64000 (JOBIN YVON) and KOMPACT MALDI IV (Shimadzu), respectively.

Contents of nitrogen and hydrogen were determined using a gas chromatographic CHN analyzer (Yanagimoto MT-3). The contents of metals were determined with an ICP spectrometer (Shimadzu ICPS 2000). It was confirmed that the content of Mo in (I) was 52 wt% and in good agreement with 52 wt% obtained from the weight of MoO₃ formed by heating (I) up to 500 °C in air. The formation of MoO₃ was confirmed by XRD. In the same way, the good agreement of the content of W measured by ICP analysis and that measured by the heat treatment was observed for (II).

Numbers of ammonia were quantitatively analyzed by using indophenol as follows:⁴³⁾ 20–100 mg of sample was solved in aqueous KOH solution (40 wt%) and this solution was heated. Ammonia evolved was trapped in aqueous H₂SO₄ solution (1 M). To this solution, aqueous solutions containing phenol and sodium nitroprusside were added. Then aqueous solutions containing sodium hydroxide and sodium hypochlorite were added and the resulting solution was kept for 3 h. The blue color developed and the absorption at 630 nm was measured with a Perkin–Elmer UV-vis spectrometer (Lambda 12). Numbers of peroxy group O₂^{2–} and proton were quantitatively analyzed by using KMnO₄ and aqueous NaOH reagents, respectively.

Proton Conductivity. Conductivity measurements were carried out for a film (300–800 nm in thickness) on a borosilicate glass substrate with a pair of interdigital sputtered Au electrodes on the surface. Sample films were prepared by a spin coat method. Proton conductivity of films was evaluated by the ac impedance method between 1 and 500 kHz using an impedance analyzer (Solartron SI-1260) in a compartment kept at the desired temperature and humidity.

Results and Discussion

Starting Metal Nitrides. The data of structure and elemental analysis for metal nitrides are summarized in Table 1. It was confirmed that the structures of nitrides of metals of Mo, V, and Ti were cubic Mo₂N (with a trace amount of Mo metal), VN, and TiN, respectively. The values of atomic ratio of N/Mo, N/V, and N/Ti were 0.50, 1.00, and 1.00, respectively, which well agreed with the stoichiometric ratio

Table 1. Data of Structure and Elemental Analysis for Metal Nitrides

M in metal (M) nitride	Structure ^{a)}	Elemental analysis ^{b)} /wt%		Atomic ratio of N/M
		M	N	
Mo	Cubic Mo ₂ N (Trace Mo)	92.8	7.1	0.52
		(93.2)	(6.8)	
W	Amorphous	95.8	4.2	0.58
		(96.3) ^{c)}	(3.7) ^{c)}	
V	Cubic VN	78.4	21.6	1.00
		(78.4)	(21.6)	
Ti	Cubic TiN	77.4	22.6	1.00
		(77.4)	(22.6)	

a) By XRD. b) Numbers in parentheses were calculated values based on the structures confirmed by XRD. c) Calculated on the assumption that the structure is W₂N.

of Mo₂N, VN, and TiN, respectively. It was confirmed for nitrides of molybdenum and tungsten that the content of hydrogen was ≤0.04% and that metallic impurity was ≤0.1%.

Reaction of Metal Nitrides with Hydrogen Peroxide (Step (1)). Peroxometalates Species. Figure 1a shows the ⁹⁵Mo NMR spectrum of the reaction solution of molybdenum nitride with hydrogen peroxide after 1 h. The spectrum changed little after 24 h. The spectrum showed a signal at –199 ppm (Δν_{1/2}, ca. 700 Hz), which is assigned to [MoO(O₂)₂(OOH)]₂^{2–}.⁴⁴⁾ Figure 1b shows the ¹⁸³W NMR spectrum of the reaction solution of tungsten nitride with hydrogen peroxide after 1 h. The spectrum changed little after 24 h. The spectrum showed two signals at –643 and –697 ppm with the intensity ratio of 0.2 : 1.0, respectively. The former signal is assigned to [WO₂(O₂)₂]^{2–}, [WO(O₂)₂(OH)][–],

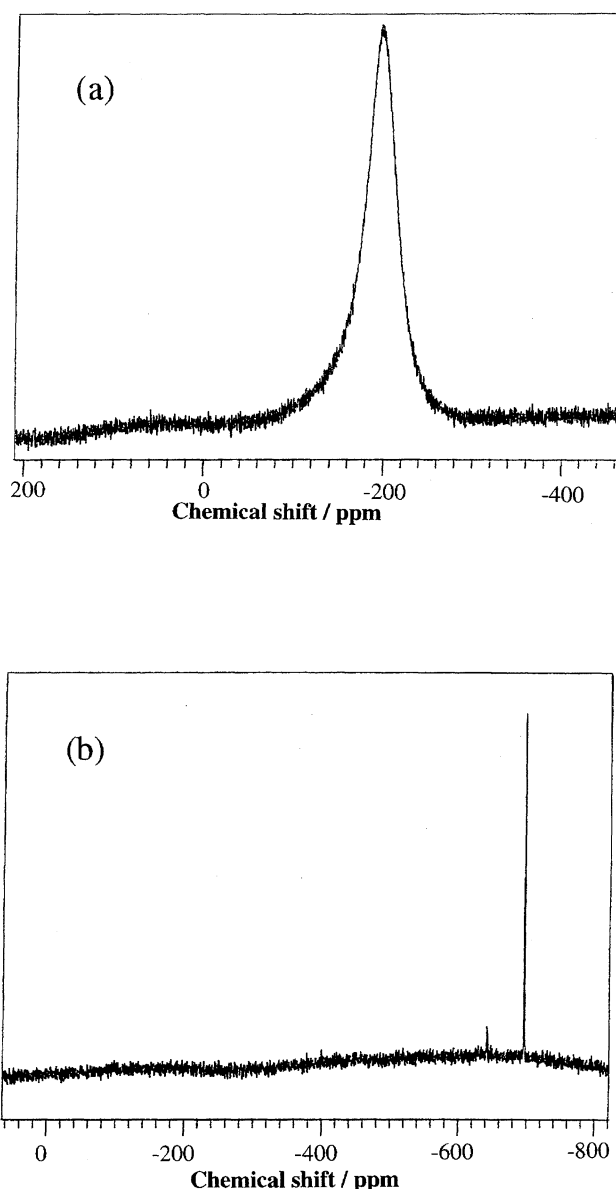


Fig. 1. ⁹⁵Mo and ¹⁸³W NMR spectra of reaction solution of nitrides of molybdenum and tungsten with hydrogen peroxide after 1 h. (a) molybdenum nitride; (b) tungsten nitride.

and/or the protonated species according to Ref. 45. The latter intense signal is assigned to $[\text{W}_2\text{O}_3(\text{O}_2)_4(\text{H}_2\text{O})_2]^{2-}$.⁴⁶⁾

Thus, in the case of the reaction of nitrides of tungsten and molybdenum, peroxodimer was mainly formed by the reaction with hydrogen peroxide. The absence of change of NMR spectra between 1 and 24 h is consistent with the fact that pH values for the reaction solution of nitrides of tungsten and molybdenum initially decreased and became almost constant after 1 h. (These facts show that the reactions of nitrides of tungsten and molybdenum were almost completed after 1 h.)

Nitrogen Species. The ^{14}N NMR spectrum of the reaction solution of nitrides of molybdenum and tungsten with hydrogen peroxide after 1 h showed one signal at ca. 20 ppm, which is assigned to ammonium ion.⁴⁷⁾ After 24 h, the signal due to nitrate ion⁴⁷⁾ was additionally observed at ca. 377 ppm.

Reaction Mechanism. No reaction occurred in the absence of hydrogen peroxide, showing that hydrogen peroxide is essential for the reaction of nitrides of Mo and W. No nitrogen species were found for the reaction solution of Mo, W, V, and Ti metals with hydrogen peroxide, showing that ammonium and nitrate ions come from N in these nitrides. In solution, ammonium and nitrate ions and peroxometalates as well as protons were formed. In the gas phase, dinitrogen and dioxygen were formed. These facts show the progress of reaction of metal nitrides with hydrogen peroxide and decomposition of hydrogen peroxide.

A trace amount of ammonium ion was detected with ^{14}N NMR after 7 d and no nitrate ion was detected when the reaction of molybdenum nitride with proton was carried out by the addition of hydrochloric acid to adjust pH to 2.0 (without hydrogen peroxide), which was the same as that of the final pH of the reaction solution with hydrogen peroxide. Only the ammonium ions were formed by the reaction of tungsten nitride in the presence of hydrochloric acid. These facts suggest that protons formed by the reaction of metal nitrides with hydrogen peroxide take part in the formation of ammonium ion, as has been reported in organometallic molybdenum nitride.⁴⁰⁾

On the basis of above results, nitrate ion may be formed by (i) the successive oxidation of ammonium ion to nitrate ion as the oxidation of aromatic amine can proceed with hydrogen peroxide and/or (ii) the oxidation of interstitial nitrogen by the peroxometalates formed in-situ.

Formation of Powder Samples (I)—(IV) (Step (2)) and

Characterization. Table 2 summarizes the data of XRD, elemental analysis, titration of NH_3 and O_2^{2-} , and ^{14}N NMR. (I)—(IV) were amorphous and therefore, we attempted various analyses.

Peroxopolymetalate Species. The chemical species in (I)—(III) were investigated. The positive TOF mass spectrum of (I) in the range of m/z 1000—5000 gave the most intense peak at 1486 ± 5 , which may correspond to peroxooctamolybdate on the basis of the data in Table 2. Subsequent loss of MoO_3 fragment is the other dominant feature and resulted in the peak at 1342. The formation of peroxooctamolybdate ion was also reported by Trysberg and Stomberg.⁴⁸⁾ The Raman spectrum of (I) showed the bands at 970s, 870w, 815vs, 660m, 565m, 370w, 330m, and 295s cm^{-1} in the range of 200—1400 cm^{-1} and was different from those of previously known peroxoisopolymolybdates of $[\text{Mo}_2\text{O}_3(\text{O}_2)_4(\text{H}_2\text{O})_2]^{2-}$, $[\text{Mo}_3\text{O}_7(\text{O}_2)_4]^{4-}$, $[\text{Mo}_7\text{O}_{22}(\text{O}_2)_2]^{4-}$, and $[\text{Mo}_{10}\text{O}_{22}(\text{O}_2)_{12}]^{8-}$.⁴⁶⁾ The fact is consistent with the formation of peroxooctamolybdate.

The TOF-MASS spectra of (II) and (III) showed the most intense peak at $|m/z|$ of 2853 and 1116, respectively in the range of 1000—4000. These mass numbers and the data in Table 2 suggest the formation of dodecatungstate and decavanadate ions, respectively. The formation of dodecatungstate well agrees with the radial distribution analysis data previously reported.⁴⁹⁾ Raman spectrum of (II) showed the bands at 1040m, 962vs, 870s, 697w, 622w, 594w, 547s, and 310s cm^{-1} in the range of 200—1400 cm^{-1} and was different from those of peroxoditungstate of $[\text{W}_2\text{O}_3(\text{O}_2)_4(\text{H}_2\text{O})_2]^{2-}$.⁴⁶⁾

Thus, the removal of unreacted hydrogen peroxide resulted in the formation of more polymerized species (I)—(III). The progress of the polymerization by the decomposition of hydrogen peroxide is consistent with the depolymerization of peroxopolymolybdates, peroxopolytungstates and peroxoniobium-containing anions by the addition of excess hydrogen peroxide.^{50–52)}

Empirical Formula of (I). The $\text{H}^+/\text{(I)}$ ratio determined by acid/base titration was 8. The number of waters in (I) was determined to be 3.0 by TGA analysis. The large $\Delta\nu_{1/2}$ in Fig. 2a and the fact that no signals due to NH_4NO_3 were observed by XRD suggest an interaction of NH_4^+ and NO_3^- ions with peroxoisopolymolybdate formed. X.p. spectrum of (I) in Mo3d region consist of an Mo3d3/2 and Mo3d5/2 doublet, 236.4 and 232.8 eV, respectively, in agreement with those reported for Mo^{6+} .⁵³⁾ On the basis of

Table 2. Data of Yields, Structure, Elemental Analysis, ^{14}N NMR, Titration, and XRD for (I)—(IV)

Sample	Yield %	Structure	Element ^{a)} /wt%			Atomic ratio of N/M	Ratio of $\text{NH}_4^+/\text{NO}_3^-$ ^{b)}	Amount ^{c)} /wt%	
			M	N	H			NH_3	O_2^{2-}
I	88	Amorphous	52	1.6	2.1	0.21	1.2	0.92	18.4
II	85	Amorphous	63	3.2	1.8	0.67	1.7	2.12	4.8
III	16	Amorphous	38	8.2	3.0	0.79	2.8	7.39	0.0
IV ^{d)}	6	Amorphous	45	6.1	3.0	0.47	1.0	— ^{d)}	— ^{d)}

a) Elemental analysis. b) Integrated ^{14}N NMR signal intensity ratios. c) Measured by titration with indophenol and KMnO_4 reagents, respectively. d) As-prepared sample was only slightly soluble in water and therefore, the titration could not be possible.

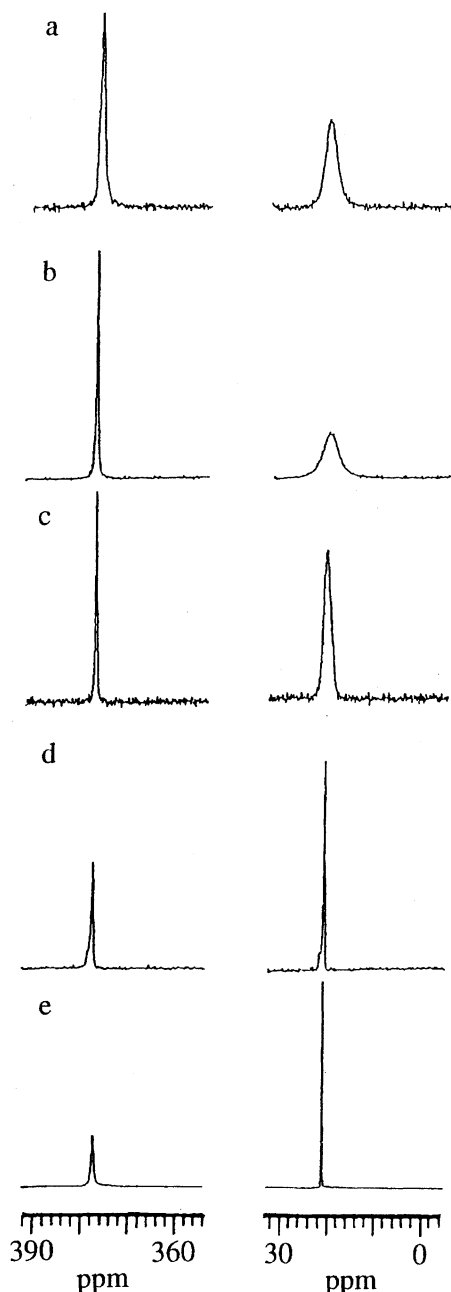


Fig. 2. ^{14}N NMR spectra of (I)–(IV). (a)–(e) are spectra of (I)–(IV), and ammonium nitrate, respectively.

the above facts, the empirical formula of (I) may be $H_8(NH_4)Mo_8O_{20}(O_2)_8(NO_3)(H_2O)_3$. This is the dominant species in (I) since the intensity of the TOF mass peak at 1486 was about 70% of the sum of the mass peaks above $-m/z=1450$.

Nitrogen Species. Next, the state of nitrogen was investigated. The data of elemental analysis show that nitrogen is included in samples (I)–(IV). The N/M atomic ratios decreased from those of metal nitrides in Table 1. For example, the N/Mo atomic ratio of (I) was 0.21 and decreased from 0.5 of starting molybdenum nitride. These decrease were due to the formation of dinitrogen, which was confirmed by gas chromatography. Figures 2a–2d and 2e show ^{14}N NMR spectra of (I)–(IV) and NH_4NO_3 , respectively. NH_4NO_3

showed two peaks at 20.7 and 377.0 ppm with the stoichiometric intensity ratio of 1.0:1.0, which are assignable to NH_4^+ and NO_3^- , respectively.⁴⁷⁾ The spectra of (I)–(IV) showed two broad peaks at 20.6–20.9 and 377.2–377.5 ppm, which are assignable to NH_4^+ and NO_3^- , respectively. No signals due to N_2H_4 and NO_2^- were seen. For example, (I) gave peaks at 20.8 ($\Delta\nu/2$, ca. 100 Hz) and 377.5 (35 Hz) ppm with an intensity ratio of 1.2:1, respectively. In addition, the amount of NH_3 (0.76 wt% as N) obtained by the titration with an indophenol reagent approximately agreed with that (0.87 wt% as N) calculated by $\{ \text{the content of N in (I)} \} \times \{ I_{NH_4^+} / (I_{NH_4^+} + I_{NO_3^-}) \}$, where $I_{NH_4^+}$ and $I_{NO_3^-}$ express the integrated ^{14}N signal intensities of NH_4^+ and NO_3^- , respectively. The agreement shows that the two peaks at 20.8 and 377.5 ppm include almost all the nitrogen atoms in (I). Similar close agreements of the amounts of ammonia obtained by the titration with those calculated based on data of elemental analysis and NMR were confirmed for (II)–(III). Thus, the present results show that nitrogen in (I)–(IV) exists as nitrate and ammonium ions.

The presence of ammonium and nitrate ions was also confirmed by IR. Figure 3a shows the IR spectrum of (I). In the range of 1300–1600 cm^{-1} , the IR spectrum showed a 1402 cm^{-1} band and a 1324 cm^{-1} shoulder, which are assigned to $\delta(NH_4^+)$ and $\nu(NO_3^-)$, respectively.^{54,55)} As summarized in Table 3, the bands due to $\delta(NH_4^+)$ and $\nu(NO_3^-)$ were also observed for (II)–(IV). No bands due to $\delta(NH_4^+)$ and $\nu(NO_3^-)$ were observed for the sample prepared by the reaction of molybdenum metal with hydrogen peroxide in Fig. 3b.

The XPS results for (I) were also consistent with the formation of NH_4^+ and NO_3^- ions. The spectrum of (I) in N1s region shows signals at 402.2 and 406.3 eV assigned to NH_4^+ and NO_3^- , respectively.⁵⁶⁾

Thus, the elemental analysis, NH_3 titration, and IR, Raman, NMR, and x.p. spectroscopy show the formation of NO_3^- and NH_4^+ ions by the reaction of nitrides of molyb-

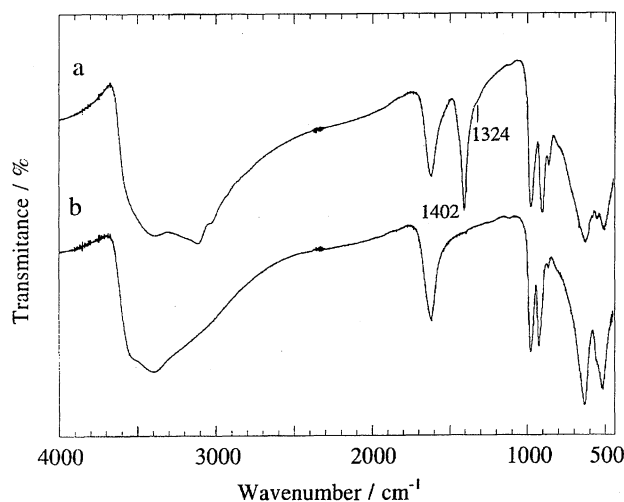


Fig. 3. Infrared spectra of samples prepared from molybdenum nitride and molybdenum metal. (a) (I); (b) powder sample prepared by the reaction of molybdenum metal with hydrogen peroxide.

Table 3. IR Bands Assigned to $\delta(\text{NH}_4^+)$ and $\nu(\text{NO}_3^-)$

Sample	Band position/ cm^{-1}	
	$\delta(\text{NH}_4^+)$	$\nu(\text{NO}_3^-)$
I	1402	1324
II	1400	1320
III	1413	1327
IV	1406	1340

denum, tungsten, vanadium, and titanium with hydrogen peroxide.

Thermal Stability. The change of (I)–(III) with the thermal treatment is investigated because the thermal stability is important for the application. The change was traced by IR spectroscopy. By the heat treatment of (I) in air, the bands of $\delta(\text{H}_2\text{O})$ and $\nu(\text{NO}_3^-)$ completely disappeared at 170 °C, followed by the disappearance of the $\delta(\text{NH}_4^+)$ band at 240 °C. Finally, MoO_3 was formed above 320 °C. The disappearance temperatures for (I)–(III) are summarized in Table 4. Sample (II) was the most stable among (I)–(III) and provided a homogeneous thin film, as described in the next section. Therefore, the protonic conductivity was measured.

Proton Conductivity. Microscopic observation of (I)–(IV) showed that only film prepared from (II) had a smooth surface without microstructures, cracks, and pinholes even after heat-treatment. The solubility of samples (I)–(IV) in water and the gelation by hydrolysis affect the fabrication and the properties of thin films. A complex impedance plot (Cole–Cole plot) of the film prepared from (II) consisted of a slightly depressed semicircle at the high frequency region and a straight line with a slope of 45°, as shown in Fig. 4. That is typically seen in measurements of proton conductors with a blocking electrode.^{26,57)} The decrease in the determined conductivity to less than $10^{-8} \text{ S cm}^{-1}$ owing to the polarization was observed, when the conductivity was measured by a d.c. method. The conductivity by ac impedance measurement was of the order of $10^{-4} \text{ S cm}^{-1}$; hence the transport number of ion was more than 99.99%. The increase in conductivity with the increase in the relative humidity (RH) suggests that charge carriers are protons. The specific conductivity (σ) was determined from the relationship, $\sigma = d/[(2n-1)Rtw]$, where R , t , d , n , and w are the observed resistance (the diameter of the semicircle), thickness of the film, distance between a pair of fingers, number of pairs of fingers, and length of a finger of the interdigital electrodes, respectively.

Table 4. Temperature of Disappearance of IR Bands of $\delta(\text{H}_2\text{O})$, $\delta(\text{NH}_4^+)$, and $\nu(\text{NO}_3^-)$

Sample	Temperature of disappearance/°C		
	$\delta(\text{H}_2\text{O})$	$\delta(\text{NH}_4^+)$	$\nu(\text{NO}_3^-)$
I	170	240	170
II	305	430	240
III	250	350	210

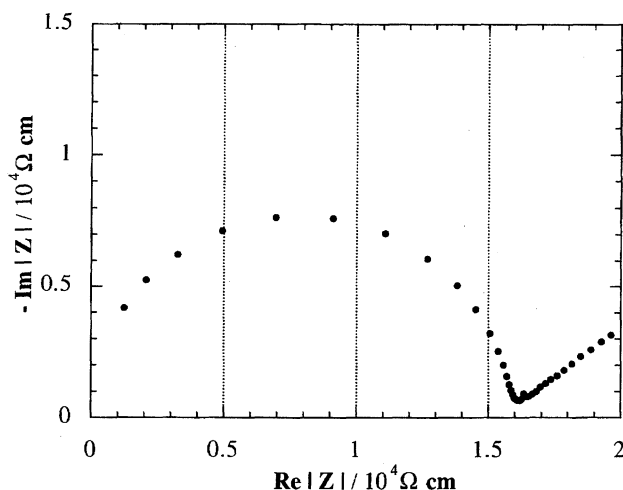


Fig. 4. Cole–Cole plot of the film of (II). Sample film was pretreated at 80 °C. Measurements were carried out at 20 °C under relative humidity of 40%.

The results showed protonic conductivity of 6.2×10^{-5} , 8.3×10^{-5} , 1.1×10^{-4} , 1.9×10^{-4} , and $2.5 \times 10^{-4} \text{ S cm}^{-1}$ at 19.7, 24.7, 29.6, 39.9, and 45.0 °C, respectively, at RH of 40%, and the logarithm of conductivity linearly changed with the inverse of absolute temperature. The linear change was due to the thermal stability and in contrast with the discontinuous change observed for high proton conductive crystals such as 12-tungstophosphoric acid^{58–60)} or uranyl hydrogenphosphate,⁶¹⁾ this was due to dehydration of these samples at elevated temperatures. The values of conductivity at 25 °C were 1.0×10^{-5} , 4.9×10^{-5} , 7.8×10^{-5} , 1.1×10^{-4} , and $3.4 \times 10^{-4} \text{ S cm}^{-1}$ at RH of 6.0, 22.0, 42.2, 59.2, and 85.2%, respectively, and the logarithm of conductivity changed approximately linearly with RH. These characteristics are important for the applications to a humidity sensors, electrolytes of electrochromic displays and so on.

We gratefully acknowledge Prof. Y. Mizobe (The University of Tokyo) for the detailed information of the titration of ammonia. This work was supported by Grant-in-Aid for Scientific Research in Priority Areas (No. 260) from The Ministry of Education, Science, Sports and Culture.

References

- 1) N. E. Brese and M. O'Keeffe, *Struct. Bonding (Berlin)*, **79**, 307 (1992).
- 2) R. Metselaar, *Pure Appl. Chem.*, **66**, 1815 (1994).
- 3) D. H. Gregory, M. G. Barker, P. P. Edwards, and D. J. Siddons, *Inorg. Chem.*, **35**, 7608 (1996).
- 4) D. H. Gregory, M. G. Barker, P. P. Edwards, and D. J. Siddons, *Inorg. Chem.*, **34**, 3916 (1995).
- 5) D. A. Vennos, M. E. Badding, and F. J. DiSalvo, *Inorg. Chem.*, **29**, 4059 (1990).
- 6) L. F. Toth, "Transition Metal Carbides and Nitrides," Academic, New York (1971).
- 7) A. E. Michale (General editor), "Borides, Carbides, and Nitrides," American Ceramic Society, Washington D. C. (1994).
- 8) R. Freer, "The Physics and Chemistry of Carbides, Nitrides,

and Borides," Kluwer Academic Pub., The Hague (1990).

- 9) Y. Xie, Y. Qian, W. Wang, S. Zhang, and Y. Zhang, *Science*, **272**, 1926 (1996).
- 10) Y. W. Bae, W. Y. Lee, C. S. Yust, P. J. Blau, and T. M. Besmann, *J. Am. Ceram. Soc.*, **79**, 819 (1996).
- 11) M. J. Kim, D. M. Brown, and W. Katz, *J. Electrochem. Soc.*, **130**, 1199 (1983).
- 12) T. Nakajima, K. Watanabe, and N. Watanabe, *J. Electrochem. Soc.*, **134**, 3175 (1987).
- 13) H. Topsøe, B. S. Clausen, and F. E. Massoth, "Catalysis," Springer, Heidelberg (1996), Vol. 11, p. 109.
- 14) M. Nagai and S. Omi, *Sekiyu Gakkaishi*, **38**, 363 (1995).
- 15) S. T. Oyama, *Catal. Today*, **15**, 179 (1992).
- 16) L. Volpe and M. Boudart, *J. Phys. Chem.*, **90**, 4878 (1986).
- 17) S. Ramanathan and S. T. Oyama, *J. Phys. Chem.*, **99**, 16365 (1995).
- 18) H. J. Lee, J.-G. Choi, C. W. Colling, M. S. Mudholkar, and L. T. Thompson, *Appl. Surf. Sci.*, **89**, 121 (1995).
- 19) Y. Zhang, Z. Wei, W. Yan, P. Ying, C. Ji, X. Li, Z. Zhou, X. Sun, and Q. Xin, *Catal. Today*, **30**, 135 (1996).
- 20) T. Kudo, *Nature*, **312**, 537 (1984).
- 21) K. Hinokuma, K. Ogasawara, A. Kishimoto, S. Takano, and T. Kudo, *Solid State Ionics*, **53–56**, 507 (1992).
- 22) T. Kudo, H. Okamoto, K. Matsumoto, and Y. Sasaki, *Inorg. Chim. Acta*, **111**, L27 (1986).
- 23) M. Hibino, M. Ugaji, A. Kishimoto, and T. Kudo, *Solid State Ionics*, **79**, 239 (1995).
- 24) M. Echigo and T. Kudo, "1994-fall Meeting of Electrochemical Soc. (Japan)," Abstr., p. 123.
- 25) N. Mizuno, H. Nakajima, H. Tanaka, and T. Kudo, *Chem. Lett.*, **1997**, 521.
- 26) H. Okamoto, K. Yamanaka, and T. Kudo, *Mater. Res. Bull.*, **21**, 551 (1986).
- 27) M. Hibino, H. Nakajima, T. Kudo, and N. Mizuno, *Solid State Ionics*, **100**, 211 (1997).
- 28) T. Kudo, A. Ishikawa, H. Okamoto, K. Miyauchi, F. Murai, K. Mochiji, and H. Umezaki, *J. Electrochem. Soc.*, **134**, 2607 (1987).
- 29) Y. M. Li, Y. Aikawa, A. Kishimoto, and T. Kudo, *Electrochim. Acta*, **39**, 807 (1994).
- 30) Y. M. Li and T. Kudo, *J. Electrochem. Soc.*, **142**, 1194 (1995).
- 31) Y. M. Li and T. Kudo, *Solar Energy Mater. Solar Cells*, **39**, 179 (1995).
- 32) J. Oi, A. Kishimoto, and T. Kudo, *J. Solid State Chem.*, **96**, 13 (1992).
- 33) J. Oi, A. Kishimoto, and T. Kudo, *J. Solid State Chem.*, **103**, 176 (1993).
- 34) X.-L. Xu and J. R. Gunter, *Solid State Ionics*, **74**, 1 (1994).
- 35) X.-L. Xu and J. R. Gunter, *Solid State Ionics*, **76**, 221 (1995).
- 36) K. Tatsumi, M. Hibino, and T. Kudo, *Solid State Ionics*, **96**, 35 (1997).
- 37) I. Takahashi, M. Hibino, and T. Kudo, *Jpn. J. Appl. Phys.*, **35**, L438 (1996).
- 38) C. J. Brinker and G. W. Scherer, "Sol-Gel Science," Academic Press, New York (1990).
- 39) D. Sellmann and B. Seubert, *Angew. Chem., Int. Ed. Engl.*, **31**, 205 (1992).
- 40) D. Sellmann, B. Seubert, M. Moll, and F. Knoch, *Angew. Chem., Int. Ed. Engl.*, **27**, 1164 (1988).
- 41) T. Adachi, D. L. Hughes, S. K. Ibrahim, S. Okamoto, C. J. Pickett, N. Yabanouchi, and T. Yoshida, *J. Chem. Soc., Chem. Commun.*, **1995**, 1081.
- 42) T. Takahashi, Y. Mizobe, M. Sato, Y. Uchida, and M. Hidai, *J. Am. Chem. Soc.*, **102**, 7461 (1980).
- 43) M. W. Weatherburn, *Anal. Chem.*, **39**, 971 (1967).
- 44) V. Nardello, J. Marko, G. Vermeersch, and J. M. Aubry, *Inorg. Chem.*, **34**, 4950 (1995).
- 45) H. Nakajima, T. Kudo, and N. Mizuno, *Chem. Lett.*, **1997**, 693.
- 46) N. J. Campbell, A. C. Dengel, C. J. Edwards, and W. P. Griffith, *J. Chem. Soc., Dalton Trans.*, **1989**, 1203.
- 47) G. C. Levy and R. L. Lichter, "Nitrogen-15 Nuclear Magnetic Resonance Spectroscopy," John Wiley & Sons, New York (1979).
- 48) L. Trysberg and R. Stomberg, *Acta Chim. Scand., A*, **35**, 823 (1981).
- 49) T. Nanba, S. Takano, I. Yasui, and T. Kudo, *J. Solid State Chem.*, **90**, 47 (1991).
- 50) M. T. Pope, *Prog. Inorg. Chem.*, **39**, 181 (1991).
- 51) R. G. Finke and M. W. Droegge, *J. Am. Chem. Soc.*, **106**, 7274 (1984), and Ref. 11 therein.
- 52) V. W. Day, W. G. Klemperer, and C. Schwartz, *J. Am. Chem. Soc.*, **109**, 6030 (1987).
- 53) D. Briggs and M. P. Seah, "Practical Surface Analysis by Auger and X-Ray Photoelectron Spectroscopy," John Wiley & Sons, New York (1983).
- 54) K. Nakamoto, "Infrared and Raman Spectra of Inorganic and Coordination Compounds," 3rd ed, Wiley Interscience, New York (1978).
- 55) C. C. Addison and D. Sutton, *Adv. Inorg. Chem.*, **8**, 195 (1967).
- 56) R. L. Chin and D. M. Hercules, *J. Phys. Chem.*, **86**, 3079 (1982).
- 57) R. C. T. Slade and G. P. Hall, *Solid State Ionics*, **35**, 29 (1989).
- 58) O. Nakamura, T. Kodama, I. Ogino, and Y. Miyake, *Chem. Lett.*, **1979**, 17.
- 59) O. Nakamura, I. Ogino, and T. Kodama, *Solid State Ionics*, **3/4**, 347 (1981).
- 60) R. C. T. Slade, J. Barker, and H. A. Pressman, *Solid State Ionics*, **28–30**, 594 (1988).
- 61) K. D. Kreuer, W. Weppner, and A. Babenau, *Solid State Ionics*, **3/4**, 353 (1981).